

Supplementary information (SI): Near interface ionic transport in oxygen vacancy stabilized cubic zirconium oxide thin films

Mohsin Raza, Simone Sanna, Lucia dos Santos Gómez, Eric Gautron, Abdel Aziz El Mel, Nini Pryds, Rony Snyders, Stephanos Konstantinidis and Vincenzo Esposito

Figure S1 shows the $^{18}\text{O}/\text{Zr}$ ratio as function of the deposition mode by the DC-sputtering at room temperature. Concentration of Zr was measured by performing RBS and NRA, considering the total concentration of Zr and O in each sample, while the O vacancy concentration was calculated for the deposited samples via the Zr/O ratio. Particularly, the concentration of Zr in the samples was measured by Rutherford back scattering (RBS). Incident energy used of the alpha particles was 2 MeV, and the beam impinged the sample surface at normal incidence. Backscattered particles were collected at 165° in a PIPS detector. Spectra were analyzed with the SIM-NRA software assuming Rutherford backscattering cross-section. In order to measure the O content in the deposited samples, ^{18}O in particular was used in the deposition for samples later used to be for elemental composition. Specific ^{18}O depth profiles were determined using the resonant nuclear reaction (NRA) $^{18}\text{O}(p,\alpha)^{15}\text{N}$ at 151 keV. During the measurement samples were tilted at 30° with respect to the incident beam and the alpha particles were collected in large area PIPS detectors facing the sample surface and parallel to it. The incident energy was varied from 145 to 200 keV. Depth profiles were deconvoluted in order to take into account the energy straggling of the beam and then quantified with the help of a Si^{18}O_2 standard produced by thermal oxidation in a pure ^{18}O atmosphere. After performing RBS and NRA on each sample, considering the total concentration of Zr and O in each sample, O vacancy concentration was thus determined for the deposited samples, as shown in the **Figure S1**. Since the concentration of oxygen vacancies in each sample is solely based on the deposition condition and not on the substrate type used, the samples deposited in the same working conditions have the same concentration of oxygen vacancies.

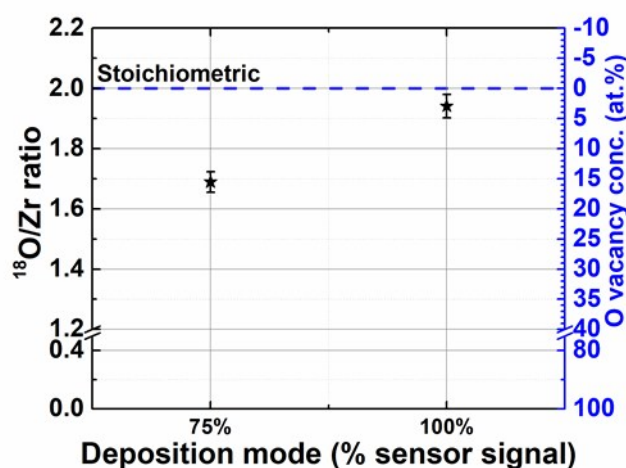


Figure S1. $^{18}\text{O}/\text{Zr}$ ratio as function of the deposition mode by the DC-sputtering at room temperature; the concentration of Zr in the samples was measured by performing RBS and ^{18}O in particular by NRA was used in the deposition for samples later used to be for elemental composition.

Figure S2 shows the microstructural features for a 2000 nm OVSZ film deposited on Si (100) and having 16 atomic % O vacancies. **Figure S2** (a) shows the overall cross-section of the OVSZ film. For the analysis of the microstructure three main regions along the deposition are distinguished and represented at higher magnification: **Figure S2** (b) near the termination (top) of the film, (c) the core cross-section and (d) the film-substrate interface. The SEM observations indicate a columnar-like growth with branched feather-like formations with an inter-columnar porosity. The morphological

features become more and more defined while moving towards the top of the film (see for example white arrows in (b) and (c)). For the near substrate/film interface region, **Figure S2** (d) indicates a rather dense microstructure for the deposition for the first 100-200 nm (in red).

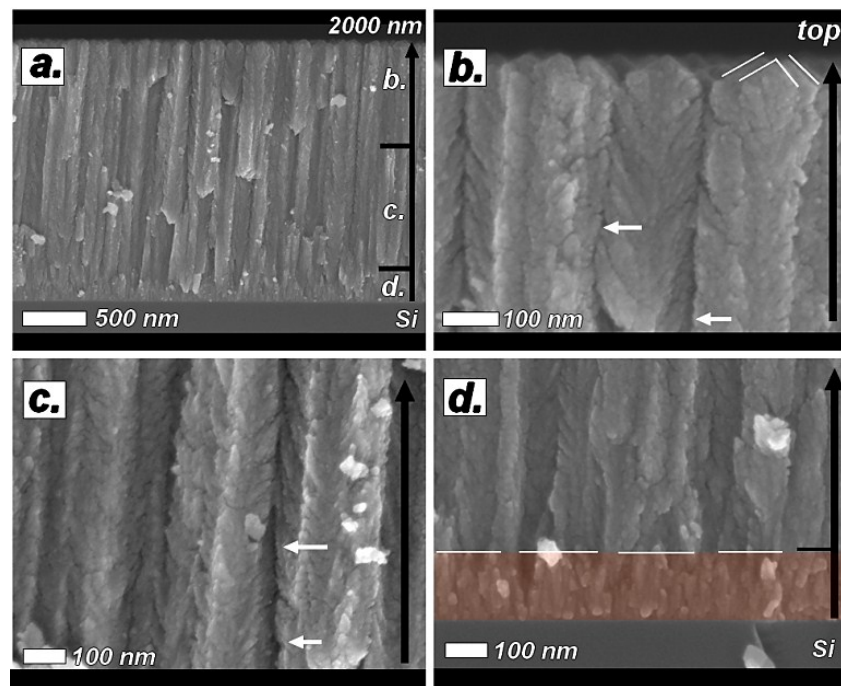


Figure S2. SEM picture of the ZrO_{2-x} thin film deposited by dc-reactive magneto sputtering at room temperature on Si showing an overall microstructure and different morphologies (c-d) developed along the thickness during the deposition.

Figure S3 shows HR-TEM indicating the change in film density and microstructure along the growth direction. It is can be seen as the “bright” regions indicating low density of film starts to appear as we approach the film surface. Moreover, it also shows the microstructure become more columnar with the increase in film thickness. **Figure S4** shows the cross-sectional images of OVSZ film. Electron diffraction performed over the whole thickness of film **Figure S3(e)** shows film has cubic crystal structure in general but above 850 nm films monoclinic crystals were found when FFT was performed at the intersection of columns.

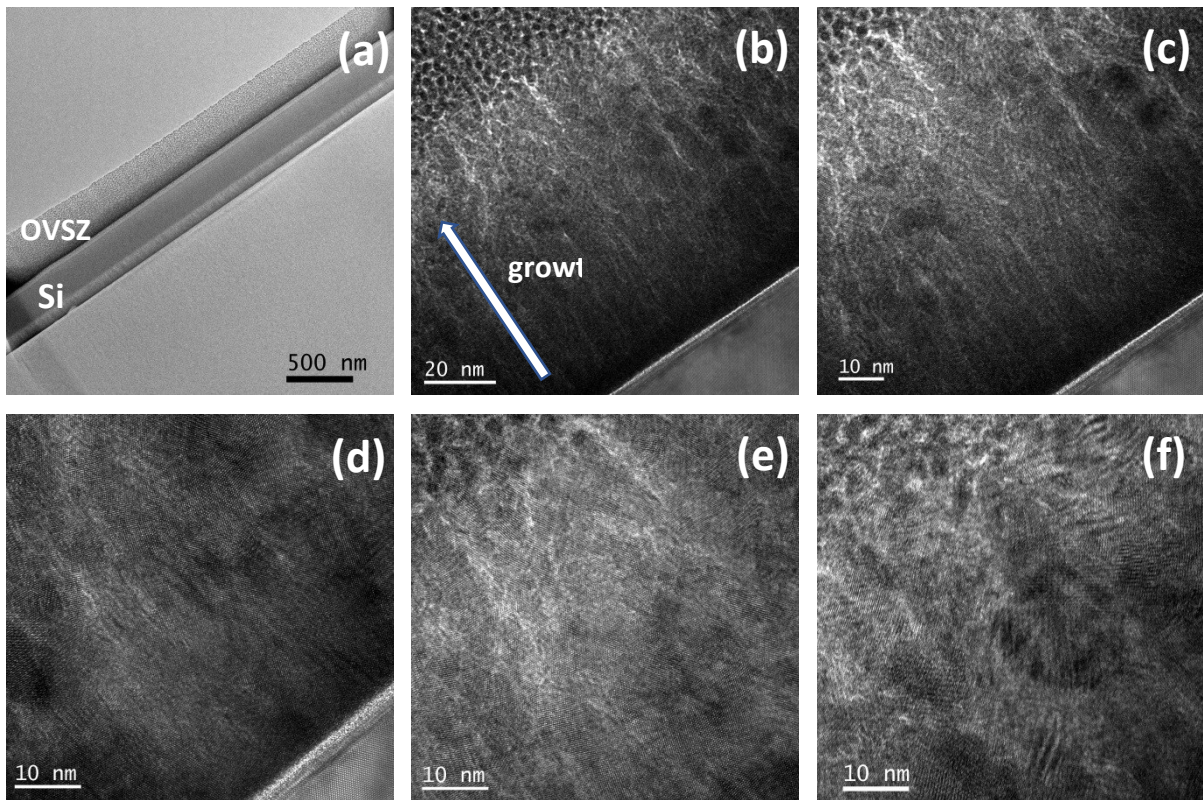


Figure S3. High resolution TEM images of OVZS thin film grown on Si substrate, (a), (b) and (c) over all view of sample, (d) near film substrate interface, (e) and (f) near the film surface termination.

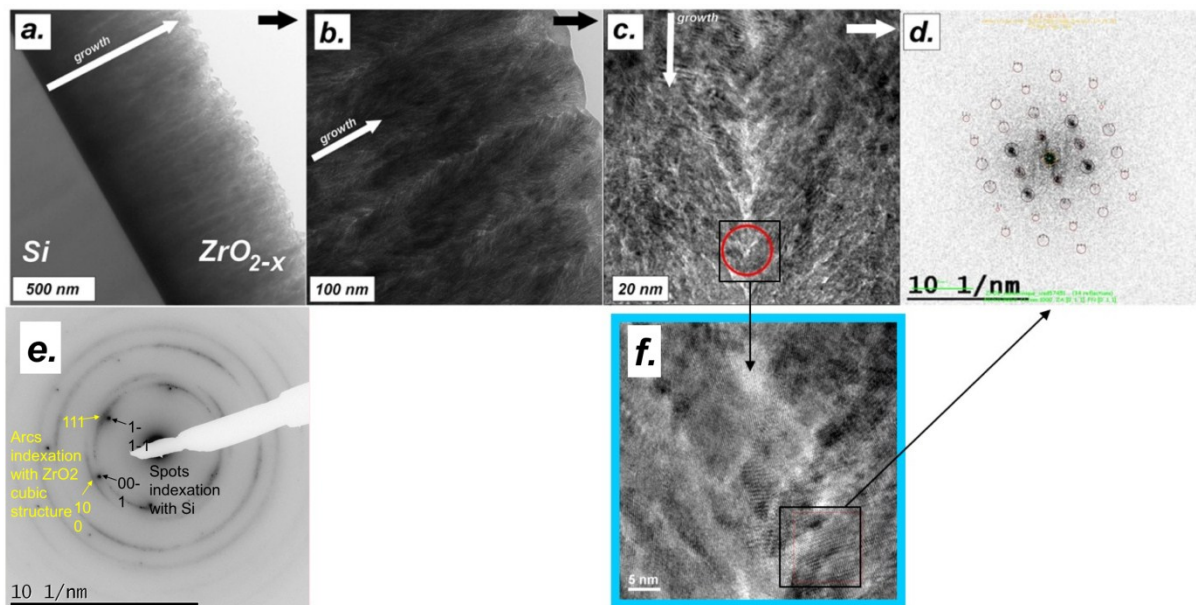


Figure S4. (a), (b) and (c) TEM images of the OVZS film. (d) FFT of the film at the intersection of columns where monoclinic crystals were found. (e) shows the electron diffraction over the whole thickness of sample having cubic crystals.

For the evaluation of the crystal structure of the samples, XRD ($\text{Cu-K}\alpha = 1.54 \text{ \AA}$) was performed on the samples deposited on Si as well as on NGO substrate. It can be seen in figure S4 that films

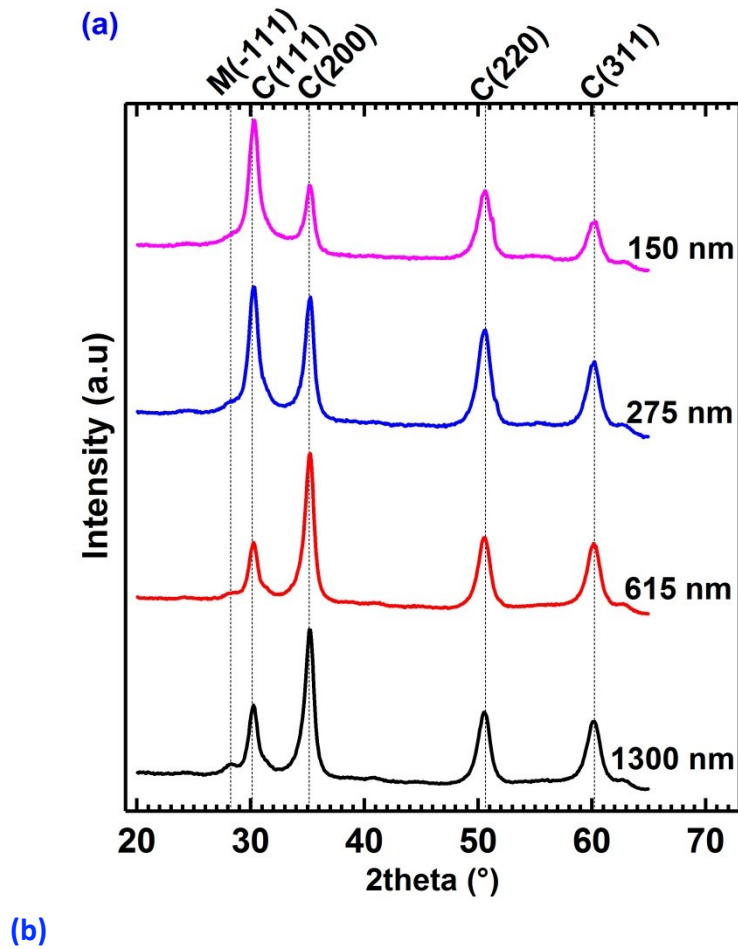


Figure S5. Shows the XRD of (a) OVSZ films on Si and (b) on NGO containing 16 at.% O vacancies.

crystallinity has no dependence on the substrate, however, it can be also seen that as the film grows thicker and reach a certain thickness (i.e. 850 nm confirmed by TEM analysis) monoclinic crystals starts to form. The overall diffraction results are consistent with HR-TEM analysis and indicate a clear prevalence of the cubic phase for low film thicknesses.

